Molecular Engineering of Photosensitizers for Nanocrystalline Solar Cells: Synthesis and Characterization of Ru Dyes Based on Phosphonated Terpyridines

S. M. Zakeeruddin, M. K. Nazeeruddin, P. Pechy, F. P. Rotzinger, R. Humphry-Baker, K. Kalyanasundaram,* and M. Grätzel*

Laboratory for Photonics and Interfaces, Institute of Physical Chemistry, Swiss Federal Institute of Technology, 1015 Lausanne, Switzerland

V. Shklover and T. Haibach

Laboratory of Crystallography, Swiss Federal Instiute of Technology, 8092 Zurich, Switzerland

Received January 3, 1997[⊗]

We report the results of an investigation on the preparation, spectral, and photoelectrochemical properties of Ru(II)−polypyridyl complexes containing a new phosphonated terpyridine (P-terpy) ligand: [Ru(H_2P-terpy)$_2$] and [Ru(HP-terpy)(Me_2bpy)(NCS)]. Resonance Raman spectral and luminescence studies allow probing into the nature of the low-energy MLCT transitions observed in these complexes. The crystal and molecular structure of the mixed-ligand complex [Ru(HP-terpy)(Me_2bpy)(NCS)] based on X-ray diffraction study is reported. This complex appears to be a promising candidate as a photosensitizer in dye-sensitized photoelectrochemical cells based on nanocrystalline films of TiO_2.

Introduction

Polypyridine complexes of Ru(II) have been the testing ground to probe many of fundamental processes governing the photoreactivity of transition metal complexes.[1,2] By varying the nature of the polypyridine ligand and introduction of different donor/acceptor/functional groups, it has been possible to "fine tune" the spectral and redox properties of theses complexes. Thus complexes have been synthesized that serve as electron donors or electron acceptors or energy transfer agents in light-induced electron transfer processes. Unlike Ru(bpy)$_3^{2+}$, the lowest excited state of the analogous complex with the tridentate terpyridine ligand, Ru(terpy)$_2^{2+}$, is practically nonluminescent and very short lived. It is desirable to identify complexes of terpyridine derivatives with better emission properties. Luminescence, though not a prerequisite for a complex to serve as a photosensitizer, helps enormously the direct measurements of excited-state properties and reactions. Of particular relevance to the present work are the recent efforts of Constable, Sauvage, and others to develop a series of oligopyridines and their derivatives (such as substituted terpyridines and quarterpyridines) as potential multidentate ligands.[3−5]

One type of application of polypyridine complexes that we have been interested for a number of years is their use as photosensitizers in photoelectrochemical solar cells.[6−8] Of particular interest are their utility in dye-sensitized solar cells based on nanocrystalline films of TiO_2.[9−11] Optical excitation using visible light of polypyridyl complexes incorporated in these nanosized membrane films leads to rapid transfer of electron from the excited state of the dye to the conduction band of the semiconductor. The oxidized form of the dye is rapidly reduced back to its ground state by redox mediators (such as iodide) present in the electrolyte separating the illuminated and counter electrode. The injected electrons diffuse through the semiconductor particles to arrive at the back-contact and then flow through the external circuit to arrive at the counter-electrode. Regeneration of the depleted redox relay leads to net conversion of visible light to electricity.

Design of efficient photosensitizers for this type of application involves considerable molecular engineering. First, the spectral absorption properties must be tuned to have maximum visible light response. Second, the redox properties of the metal complex should be tuned for the complex in the excited state to have sufficient driving force to participate in electron transfer reactions. Polypyridine complexes of transition metals have been materials of first choice in view of the extensive knowledge available on this series of complexes. Metal-to-ligand charge transfer transitions dominate their visible light absorption and much of their photophysical and redox behavior.

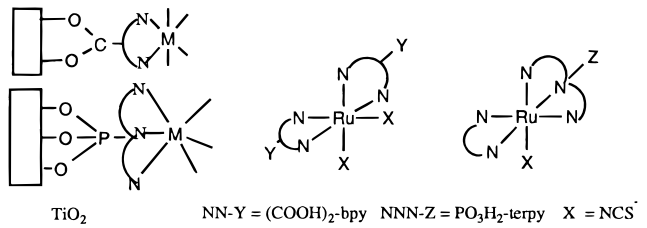

A third important factor to consider in dye design is the role of functional groups on the dye that allow efficient adsorption

⊗ Abstract published in *Advance ACS Abstracts*, November 1, 1997.

(1) (a) Kalyanasundaram, K. *Photochemistry of Polypyridine and Porphyrin Complexes*; Academic Press: London, 1992. (b) Roundhill, D. M. *Photophysics and Photochemistry of Coordination Compounds*; Wiley: New York, 1994. (c) Balzani, V.; Scandola, F. *Supramolecular Photochemistry*; Wiley: Chichester, U.K., 1991. (d) Juris, A.; Campagna, S.; Balzani, V.; Belser, P.; von Zelewsky, A. *Coord. Chem. Rev.* **1988**, *84*, 85.

(2) Kalyanasundaram. K., Grätzel, M., Eds. *Photosensitization and Photocatalysis Using Inorganic and Organometallic Compounds*; Kluwer Academic Publishers: Dordrecht, The Netherlands, 1993.

(3) Constable, E. C. *Pure Appl. Chem.* **1996**, *68*, 253; *Prog. Inorg. Chem.* **1994**, *42*, 67; *Tetrahedron* **1992**, *48*, 10013 and references cited therein.

(4) Sauvage, J.-P.; Collin, J.-P.; Chambron, J.-C.; Guillerez, S.; Coudret, V.; Balzani, V.; Barigelletti, F.; De Cola, L.; Flamigni, L. *Chem. Rev.* **1994**, *94*, 993 and references cited therein.

(5) Maestri, M.; Armaroli, N.; Balzani, V.; Constable, E. C.; Cargill Thompson, A. M. W. *Inorg. Chem.* **1995**, *34*, 2759. Barigelletti, F.; Flamigni, L.; Guardigli, M.; Sauvage, J.-P.; Collin, P.-P.; Sour, A. *J. Chem. Soc., Chem. Commun.* **1996**, 1329.

(6) DeSilvestro, J.; Grätzel, M.; Kavan, L.; Augustynski, J. *J. Am. Chem. Soc.* **1985**, *107*, 2988.

(7) Vlachopoulos, N.; Liska, P.; Augustynski, J.; Grätzel, M. *J. Am. Chem. Soc.* **1988**, *110*, 1216. Liska, P.; Vlachopoulos, V.; Nazeeruddin, Md. K.; Comte, P.; Grätzel, M. *J. Am. Chem. Soc.* **1988**, *110*, 3686.

(8) Nazeeruddin, Md. K.; Liska, P.; Moser, J.; Vlachopoulos, V.; Grätzel, M. *Helv. Chim. Acta* **1990**, *73*, 1788.

S0020-1669(97)00008-6 CCC: $14.00

on the semiconductor surface and promote electronic communication between the donor orbitals of the dye and the acceptor orbitals of the semiconductor. Earlier studies based on $[Ru(dcbpy)_3]^{2-}$, $[Ru(dcbpy)_2(NCS)_2]$, and $[(CN)Ru(bpy)_2]_2Ru(dcbpy)_2(CN)$ have unambiguously shown the utility of carboxyl groups as efficient anchoring groups. These complexes show monochromatic photon-to-current conversion efficiency of >90%. One of the problem with this class of dyes, related to the long-term stability of the solar cells, is slow desorption from the semiconductor surface in the presence of water. So a search began looking for alternate anchoring groups. In one approach we decided to examine complexes containing phosphonate groups attached either to bipyridine or terpyridine ligands.

Herein we report the results of our studies involving a number of Ru(II) complexes containing one or more of a phosphonated terpyridine, 4-phosphonato-2,2′:6,2″-terpyridine (P-terpy) as the key ligand. A description of the synthetic details of this ligand and derived complexes is first presented. This is followed by characterization of their structure and properties using a number of physical techniques, such as UV−visible and luminescence spectroscopy, cyclic voltammetry, ^1H and ^{31}P NMR, and resonance Raman spectroscopy. Direct information on the molecular and crystal structure has been obtained via X-ray diffraction studies on single crystals of one such Ru complex. A preliminary communication reporting early results on the performance of these complexes on nanocrystalline TiO_2-based solar cells has appeared earlier.[12]

Experimental Section

Materials. The chemicals 2,2′:6,2″-terpyridine, tetrakis(triphenylphosphine)palladium, and triethylamine and the solvents were commercial puriss grade chemicals from Fluka and were used as supplied. $RuCl_3 \cdot xH_2O$, puriss grade was obtained from Johnson & Matthey. 4, 4′-Dimethyl-2,2′-bipyridine (Me_2bpy) was a commercial sample from Aldrich and was recrystallized before use. For simplicity, the neutral/diprotonated form of the ligand 4-phosphonato-2,2′:6,2″-terpyridine will be referred as H_2P-terpy. Similarly, the corresponding deprotonated dianion, monoester, and diethyl ester derivatives of this ligand will be referred to as P-terpy^{2-}, EtP-terpy$^-$, Et_2P-terpy, respectively. The terpyridine ligand, their precursors, and 4-bromoterpyridine will be referred to as Br-terpy, and the diethyl ester of the phosphonated terpyridine, as Et_2P-terpy (**1**). Various Ru complexes prepared in this work will be referred to as follows (**A** and **B** refer to the ester and free acid form of the ligand in the respective complexes): homo bis chelate $[Ru^{II}(H_2P\text{-terpy})_2]^{2+}$ (**2B**), its monoester derivative $[Ru^{II}(EtP\text{-terpy})_2]^0$ (**2A**), $[Ru^{III}(Et_2P\text{-terpy})Cl_3]^0$ (**3**), $[Ru^{II}(EtP\text{-terpy})(Me_2bpy)Cl]^0$ (**4A**), $[Ru^{II}(H_2P\text{-terpy})(Me_2bpy)Cl]^+$ (**4B**), $[Ru^{II}(EtP\text{-terpy})(Me_2bpy)(NCS)]^0$ (**5A**), and $[Ru^{II}(HP\text{-terpy})(Me_2bpy)(NCS)]^0$ (**5B**).

Methods. Analytical Measurements. ^1H and ^{31}P NMR studies were made on a Bruker 220 MHz FT-NMR spectrometer. Absorption spectra were recorded on a Cary Lambda 5 UV−vis−NIR spectrophotometer. Elemental analyses of ligand and complexes were made at the central analytical laboratories of Ciba-Geigy at Basel. Mass spectral data were measured on a Finniston mass spectrometer. Cyclic voltammetric measurements were made in DMSO (containing 0.1 M tetrabutyl ammonium triflate as the support electrolyte) on a conventional three-electrode cell using glassy carbon and Pt wire as working and counter electrode, respectively. An aqueous saturated calomel electrode (SCE) was used as the reference electrode, and the redox potentials quoted are with respect to SCE. Emission spectra were recorded on a Spex Fluorolog spectrofluorimeter equipped with a Hamamatsu red-sensitive photomultiplier tube and single photon counting detection system, and the emission spectra were corrected for variations in the lamp intensity, optics, and PM spectra response.

Synthesis of the Ligand 4-Phosphonato-2,2′:6,2″-terpyridine (Et_2P-terpy) (1). 4-Bromo-2,2′:6,2″-terpyridine was prepared in 80% yield via bromination of 2,6-bis(2′-pyridyl)-4-pyridone using $POBr_3$,[13a] and the product was purified by column chromatography. The Br group was subsequently replaced by phosphonate groups using diethyl phosphite in the presence of tetrakis(triphenyl-phosphine)palladium-(0) and triethylamine as follows: 2.55 g of 4′-bromo-2,2′:6,2″-terpyridine (8.2 mmol), 0.6 g of tetrakis(triphenylphosphine)palladium (0.5 mmol), 1.9 g of diethyl phosphite (14 mmol), and 1.52 g/2.1 mL of triethylamine (15 mmol) are measured into an Ar-filled 50-mL round bottom flask, equipped with a cold finger (19 cm) and a magnetic stirrer. The mixture is heated on an oil bath at 95 °C for 3 h and cooled back to room temperature. The solidified mixture is added to 25 mL of methanol, and the solution is chromatographed on a silica gel column (gradient elution with CH_2Cl_2/CH_3OH). Evaporation to dryness of the fractions lead to isolation (1.7 g) of the diester of the desired ligand, diethyl-2,2′:6,2″-terpyridine-4-phosphonate (**1**). Unreacted starting material (0.57 g) can be recovered from earlier fractions. Yield of the desired ligand: 72.3%. Anal. Calcd for $C_{19}H_{20}N_3O_3P$ ($M_r = 369.36$): C, 61.79; N, 5.46; N, 11.38; P, 8.39. Found: C, 61.86; H, 5.42; N, 11.27; P, 8.50. MS (EI): [*m*/*e* (rel intensity)]: M^+, 369 (29.1).

Synthesis of $[Ru(EtP\text{-terpy})]_2$ (2A) and $[Ru(H_2P\text{-terpy})]_2Cl_2$ (2B). The bis(terpyridine) complex is prepared by refluxing a 1:2.2 ratio of $RuCl_3 \cdot 3H_2O$ and the ethyl ester of the phosphonated terpyridine ligand (Et_2P-terpy) in DMF for 6 h under nitrogen. The reaction mixture is cooled after this period and filtered through a sintered glass crucible. The filtrate was concentrated, and the desired complex was precipitated by addition of diethyl ether. The ^1H NMR of the isolated product showed that the complex is partially hydrolyzed $[Ru(EtP\text{-terpy})_2]^0$ (**2A**). For complete hydrolysis, the solid is dissolved in 4 N HCl and refluxed under nitrogen for 10 h. The reflux solution is allowed to crystallize at room temperature. The resulting microcrystalline solid was collected on a sintered glass crucsible and then thoroughly washed with diethyl ether and dried under vacuum. The UV−visible absorption spectrum of the complex (**2B**) in water (pH 3 or 9) shows maxima at 480, 330 sh, 310, 274, and 238 nm.

Synthesis of the Mixed-Ligand Complex [Ru(HP-terpy)(Me_2bpy)(NCS)] (5B). The desired complex was prepared by a sequential ligand replacement procedure as follows: $RuCl_3 \rightarrow [Ru(LLL)Cl_3] \rightarrow [Ru(LLL)(LL)Cl] \rightarrow [Ru(LLL)(LL)(NCS)]$, where LLL and LL denote the phosphonated terpyridine and dimethylbipyridine, respectively

Step 1: Synthesis of $[Ru^{III}(Et_2P\text{-terpy})Cl_3]$ (3). This is prepared by a slightly modified procedure of Dwyer et al.[13b] A 200 mg amount of $RuCl_3 \cdot 3H_2O$ (0.77 mmol) and 284 mg of the ligand 4′-PO_3Et_2-terpy (0.77 mmol) (**2**) were refluxed in ethyl alcohol, under nitrogen for 1 h. After this period the reaction mixture is allowed to cool and the resulting precipitate collected on a sintered glass crucible. The solid is washed thoroughly by ethyl alcohol followed by diethyl ether and dried under vacuum to give a yield of the trichloro complex (**3**) of over 90%.

Step 2: Synthesis of [Ru(EtP-terpy)(Me_2bpy)Cl] (4A). This is prepared by refluxing 200 mg of the trichloro complex $[Ru(LLL)Cl_3]$ (**3**) and 83 mg of the ligand 4,4′-dimethyl-2,2′-bipyridine (Me_2bpy) (0.45 mmol) in 20 mL of DMF for 5 h under nitrogen. The reaction mixture is cooled and filtered through sintered glass crucible. The filtrate was concentrated, and the desired complex **4A** was precipitated by addition of diethyl ether. The complex was redissolved into a small quantity of DMF and precipitated by the addition of diethyl ether. The precipitate was washed thoroughly with diethyl ether and dried under vacuum. Spectral analysis of the isolated complex indicated that partial hydrolysis had occurred at this stage and the phosphonate group is present as a monoester $[EtP\text{-terpy}]^-$. The fully hydrolyzed form of the Ru complex (**4B**) was obtained by refluxing the monochloro monoester complex (**4A**) in 4 N HCl.

Step 3: Synthesis of [Ru(EtP-terpy)(Me_2bpy)(NCS)] (5A). A 170 mg amount of the monochloro complex **4A** (0.27 mmol) is dissolved in 20 mL of DMF under nitrogen. To this solution was added 2 mL

(9) O'Regan, B.; Moser, J.; Anderson, M. A.; Grätzel, M. *J. Phys. Chem.* **1990**, *94*, 8720.
(10) O'Regan. B.; Grätzel, M. *Nature* **1991**, *353*, 737.
(11) Nazeeruddin, Md. K.; Kay, A.; Rodicio, I.; Humphry-Baker, R.; Müller, E.; Liska, P.; Vlachopoulos, N.; Grätzel, M. *J. Am. Chem. Soc.* **1993**, *115*, 6382.
(12) Pechy, P.; Rotzinger, F. P.; Nazeeruddin, M. K.; Köhle, O.; Zakeeruddin, S. M.; Humphry-Baker, R.; Grätzel, M. *J. Chem. Soc., Chem. Commun.* **1995**, 65.
(13) (a) Constable, E. C.; Ward, M. D. *J. Chem. Soc., Dalton Trans.* **1990**, 1405. (b) Dwyer, F. P.; Goodwin, H. A.; Gyarfas, F. C. *Aust. J. Chem.* **1943**, *16*, 42.

of an aqueous solution of NaNCS (300 mg, 3.7 mmol). After being refluxedfor 5 h, the mixture was cooled and filtered. The filtrate was concentrated to 5 mL on a rotovap. The desired product **5A** was precipitated out from this concentrated solution by addition of diethyl ether. The product was filtered out, washed with diethyl ether, and dried under vacuum.

Synthesis of [Ru(HP-terpy)(LL)(NCS)] (5B). To a DMF solution of complex **4B** (100 mg, 0.15 mmol) was added an aqueous solution of NaNCS (100 mg, 1.23 mmol) and refluxed for 5 h under nitrogen. The reaction mixture was cooled and filtered. The filtrate was evaparated to dryness. The resulting solid was taken in 20 mL of water and was dissolved by the addition of 0.10 M NaOH (3 mL). The solution was filtered through a sintered glass crucible. The pH of this solution was lowered to 3 by using 0.05 M HNO_3 acid or aqueous trifluromethanesulfonic acid. At this pH the complex precipitates out as a neutral salt at its isoelectric point and the flask was kept in a rtefrigerator for 12 h. The resulting precipitate was collected on a sintered glass crucible, washed thoroughly with aqueous pH solution followed by acetone, and dried under vacuum. Anal. Calcd for $C_{28}H_{23}N_6O_3PRuS\cdot 6H_2O$: C, 44.00; H, 4.58; N, 11.00%. Found: C, 44.04; H, 4.31; N, 10.87.

Single-Crystal Diffraction Study of the Complex [Ru(HP-terpy)(Me$_2$bpy)(NCS)]. The crystals of complex [Ru(HP-terpy)(Me_2bpy)(NCS)] (**5B**) were obtained from a DMSO solution on slow evaporation at room temperature. Crystal and molecular structural studies were made by X-ray diffraction using single crystals of the mixed-ligand complex **5B**. In view of the small size of the crystals used and the instability of the crystals during ambient temperature measurements (possibly loss of solvent molecules), the data collection for the single crystal **5B** was performed at 210 K on an Enraf-Nonius CAD-4 diffractometer using Mo Kα radiation ($\lambda = 0.710\ 73$ Å) equipped with a graphite monochromator. Using the $\omega/2\theta$ scan technique all reflections in the range $2° < \theta < 30°$ were collected with the CAD4-EXPRESS software.[14] The index ranges were $-10 < h < 10$, $-14 < k < 0$, and $-22 < l < 22$. Three standard reflections were measured every 1 h for the intensity control, and two standard reflections were checked every 100 reflections for the orientation control. The intensities were measured with a prescan determined scan speed to reach the ratio $\sigma(I)/I = 0.03$, and the maximum measurement time was 2 min per reflection. For the absorption correction, a ψ-scan of 9 reflections with the step $\Delta\psi = 10°$ was performed. The minimum and maximum transmission coefficients were 80.0% and 90.0%, respectively.

The structure **1** was solved by direct methods. The solvents of crystallization (one molecule of dimethyl sulfoxide and four molecules of water) were found in the general positions in the difference Fourier synthesis. As a consequence, the composition of the crystal **5B** is $C_{28}H_{23}N_6O_3PSRu\cdot(CH_3)_2SO\cdot 3.5H_2O$. The structure was refined by full-matrix least squares with anisotropic displacement parameters for the atoms Ru, P, S, O, and N, the C atoms in the terminal CH_3 groups in bpy-ligands and in the SCN group, and all atoms of the crystallization dimethyl sulfoxide and water molecules. The water oxygen atom O(8) is disordered around the inversion center at ($^1/_2$, $^1/_2$, 1) (separation O(8)$\cdots$O(8)($1-x$, $1-y$, $2-z$) of 1.41 Å) and was refined with the population 0.5. The H atoms in the complex **5B** and in the dimethyl sulfoxide molecule were placed in the idealized positions and used in the calculation of the structure factors (riding model). The hydrogen atoms of water molecules were not localized. Experimental details and results of the structure refinement are summarized in Table 1, and the atomic coordinates are given in Table 2. Programs of SHELXTL PLUS were used for data reduction, structure solution, and refinement.[15]

Preparation of Dye-Coated Nanocrystalline TiO_2 Electrodes. Nanocrystalline oxide electrodes for photoelectrochemical studies were prepared in a two step process: preparation of a colloidal solution of TiO_2 and subsequent deposition of this colloid on a conducting glass substrate. A typical synthesis of a colloid TiO_2 nanoparticles is as follows: 125 mL of Ti−isopropoxide is added dropwise and at room temperature to 750 mL of 0.1 M HNO_3 solution under vigorous stirring. A white precipitate is formed instantaneously. Immediately after hydrolysis, the slurry is heated to 80 °C and stirred vigorously for 8 h to achieve peptization. The solution is then filtered on a glass frit to remove nonpeptized agglomerates. Water is added to the filtrate to adjust the final concentration to 5% by weight. The growth of these particles up to 10−25 nm is achieved under hydrothermal conditions in a Ti autoclave heated for 12 h at 210 °C (average particle diameter 15 nm). Sedimentation takes place during the autoclaving, and the particles are redispersed using a titanium ultrasonic horn (400 W, 15 × 2 s pulses). After 2 sonications the colloidal suspension is introduced in a rotary evaporator and evaporated (35 °C, 30 mbar) to a fnal TiO_2 concentration of 11% by weight. To prevent cracking during film drying and thus render the synthesis of 10 μm thick film possible, polyethylene glycol (MW 20000, Merck) is added in a proportion of 10% of the TiO_2 weight. The resulting paste is stored in a screwed thread bottle until deposition.

Table 1. Crystal and Refinement Data for [Ru(HP-terpy)(Me_2bpy)(NCS]$\cdot(CH_3)_2SO\cdot 3.5H_2O$ (**5B**)

formula	$C_{30}H_{36}N_6O_{7.5}PS_2Ru$
M_r	796.8
cryst dimens, mm	0.04 × 0.1 × 0.03
a, Å	8.770(1)
b, Å	11.358(3)
c, Å	17.945(5)
α, deg	97.72(2)
β, deg	99.76(2)
γ, deg	96.73(2)
V, Å^3	1727.6(8)
space group	$P\bar{1}$
Z	2
d_{calc}, g·cm^{-3}	1.532
radiation (μ, cm^{-1})	graphite-monochromated Mo Kα, 0.710 73
linear abs coeff (μ, cm^{-1})	3.1
temp, °C	−60
reflcns collcd	6735
reflcns indpdt	6419
internal *R*-value	0.0589
reflcns in refinement	1877 with $F > 4\sigma(F)$
refined params	308
data/param ratio	6.1:1
final *R*, R_w[a]	0.0779, 0.0677
S	1.71
$(\Delta/\sigma)_{max}$	0.031
$\Delta\rho_{max}$, e·Å^{-3}	1.23
$\Delta\rho_{min}$, e·Å^{-3}	−0.79

[a] $R_F = \sum||F_o| - |F_c||\sum|F_o|$. $R_{wF} = [\sum w(|F_o| - |F_c|)^2/\sum w|F_o|^2]^{1/2}$.

TiO_2 electrodes by deposition of the colloidal solution of TiO_2 using a doctor blade technique on NipponSheet Glass coated with F-doped SnO_2 layer (≈85% transmission in the visible, 8−10 Ω/sq). The resulting green layer is ca. 100 μm thick. The layer is dried in air for 10 min followed by a 15 min treatment around 50 °C. The film is then heated up to 450 °C at 20−50 °C/min and left at 450 °C for 30 min before cooling to room temperature. The resulting film thickness is around 7−10 μm. Electrodes prepared using colloids autoclaved at or below 230 °C are fully transparent as the one made from colloid autoclaved above this temperature are translucent to opaque. The electrodes synthesized from particles autoclaved at 250 °C gave better photovoltaic response due to their ability to scatter light. The formation of rutile during the hydrothermal growth can be avoided by keeping the temperature lower than 240 °C.

The TiO_2 nanocrystalline electrode is immersed overnight (≈10 h) in a solution of 3×10^{-4} M of the Ru complex dissolved in ethanol. To minimize rehydration of the TiO_2 surface from moisture at ambient air (which causes dye desorption), the electrodes, while still warm (80−100 °C) from annealing, were exposed to the dye solution. The electrode is then rinsed and dried. The redox electrolyte solution used consisted of 500 mM (dimethylhexyl)imidazolinium, 20 mM of I_2, 50 mM LiI, and 500 mM *tert*-butylpyridine dissolved in acetonitrile. (In preliminary studies reported earlier, we employed a mixture of 50 mM I_2 and 500 mM KI dissolved in a 1:1 (v/v) mixture of ethylene carbonate and propylene carbonate). A sandwich-type cell was constructed by depositing a drop of an iodine-based electrolyte solution on the surface of the electrode (and let it penetrate inside the TiO_2 film by capillarity)

(14) *CAD4-EXPRESS. User Manual*; Delft Instruments X-ray Diffraction: Delft, The Netherlands, 1992.
(15) Sheldrick, G. M. *SHELXTL PLUS. VAX/VMS Version*; Siemens Analytical X-ray Instruments Inc.: Madison, WI, 1990.

Table 2. Atomic Coordinates and Equivalent Isotropic Displacement Parameters B_{eq} for **5B**

	x	*y*	*z*	B_{eq} (Å^2)
Ru	0.2985(2)	−0.1821(2)	0.3284(1)	0.0195(6)
S(1)	0.2095(8)	0.2172(5)	0.4205(3)	0.059(3)
P	0.3063(7)	0.0711(5)	0.0232(3)	0.038(2)
O(1)	0.4700(15)	0.1380(11)	0.0328(6)	0.042(5)
O(2)	0.2813(15)	−0.0344(13)	−0.0445(7)	0.057(6)
O(3)	0.1745(15)	0.1393(11)	0.0140(7)	0.050(6)
N(1)	0.2861(18)	−0.2683(13)	0.4215(8)	0.028(7)
N(2)	0.3413(17)	−0.3472(14)	0.2905(8)	0.029(6)
N(3)	0.0665(15)	−0.2297(12)	0.2760(7)	0.021(6)
N(4)	0.3021(17)	−0.1108(13)	0.2364(8)	0.023(6)
N(5)	0.5329(16)	−0.1110(13)	0.3438(8)	0.024(6)
N(6)	0.2543(16)	−0.0141(15)	0.3798(8)	0.021(6)
C(1)	0.311(2)	−0.384(2)	0.411(1)	0.025(5)
C(2)	0.283(2)	−0.4543(2)	0.468(1)	0.034(5)
C(3)	0.240(2)	−0.412(2)	0.532(1)	0.027(5)
C(4)	0.225(2)	−0.290(2)	0.546(1)	0.034(5)
C(5)	0.253(2)	−0.225(2)	0.489(1)	0.033(5)
C(6)	0.347(2)	−0.426(2)	0.338(1)	0.028(5)
C(7)	0.381(2)	−0.543(2)	0.317(1)	0.034(5)
C(8)	0.411(2)	−0.576(2)	0.245(1)	0.038(6)
C(9)	0.410(2)	−0.499(2)	0.196(1)	0.033(5)
C(10)	0.377(2)	−0.385(2)	0.223(1)	0.031(5)
C(11)	0.207(2)	−0.492(2)	0.593(1)	0.05(1)
C(12)	0.453(3)	−0.703(2)	0.228(1)	0.08(1)
C(13)	−0.052(2)	−0.294(2)	0.298(1)	0.032(5)
C(14)	−0.197(2)	−0.312(2)	0.258(1)	0.036(6)
C(15)	−0.238(2)	−0.275(1)	0.189(1)	0.029(5)
C(16)	−0.115(2)	−0.206(2)	0.164(1)	0.037(5)
C(17)	0.033(2)	−0.184(1)	0.2065(9)	0.021(4)
C(18)	0.168(2)	−0.115(1)	0.186(1)	0.024(5)
C(19)	0.163(2)	−0.060(1)	0.1193(9)	0.023(5)
C(20)	0.306(2)	−0.004(2)	0.108(1)	0.025(5)
C(21)	0.436(2)	0.003(1)	0.161(1)	0.027(5)
C(22)	0.437(2)	−0.052(1)	0.2239(9)	0.024(5)
C(23)	0.566(2)	−0.051(2)	0.288(1)	0.028(50
C(24)	0.721(2)	0.004(2)	0.290(1)	0.032(5)
C(25)	0.836(2)	−0.005(2)	0.352(1)	0.038(5)
C(26)	0.803(2)	−0.069(1)	0.406(1)	0.045(6)
C(27)	0.645(2)	−0.124(2)	0.400(1)	0.039(5)
C(28)	0.240(2)	0.080(2)	0.393(1)	0.028(8)
S(2)[a]	0.947(1)	0.3238(8)	0.2266(5)	0.108(4)
O(4)[a]	0.828(2)	0.272(2)	0.263(1)	0.13(1)
C(29)[a]	0.851(3)	0.365(3)	0.135(1)	0.14(2)
C(30)[a]	1.017(3)	0.197(2)	0.177(2)	0.13(2)
O(5)[b]	0.165(2)	−0.625(2)	0.017(1)	0.11(1)
O(6)[b]	0.117(2)	−0.393(2)	0.061(1)	0.11(1)
O(7)[b]	0.423(2)	−0.297(1)	0.0557(8)	0.080(8)
O(8)[c]	0.424(4)	0.474(3)	0.980(2)	0.10(2)

[a] Dimethyl sulfoxide molecule (solvent of recrystallization). [b] Water molecule (water of hydration). [c] Water molecule, refined with population 0.5 (water of hydration).

and clipping on top of the TiO_2 electrode with a platinized counter electrode. The dye-coated TiO_2 film was then illuminated through the transparent conducting glass support. Illumination area of the cell is typically 6 mm × 6 mm. An Oriel 150 W Xe arc lamp, equipped with Oriel 51942 and Oriel AMO optical filters, was used as the light source for solar light simulations (AM 1.5). The light power was measured using a YSI-Kettering 65A radiometer. The UV−vis absorption spectra were measured on Cary Lambda 5 UV−vis−near-IR spectrophotometer. The conversion efficiency (incident monochromatic photon-to-current conversion efficiency (IPCE)) are overall yields uncorrected for losses due to light absorpiton and reflection by the conducting glass support.

Results and Discussion

1. Synthesis. Scheme 1 shows the details of the synthetic strategy adopted for the synthesis of the key ligand 4-phosphonato-2,2′:6,2″-terpyridine (P-terpy). The ligand was prepared from 4-bromoterpyridine by a modification of Hirao's procedure[16] for the synthesis of pyridine-3-phosphonic acid diethyl ester. The ligand was isolated as the diethyl ester (Et_2P-terpy) and used as such.

Scheme 1. Synthetic Scheme for the Preparation of the Phosphonated Terpyridine Ligand

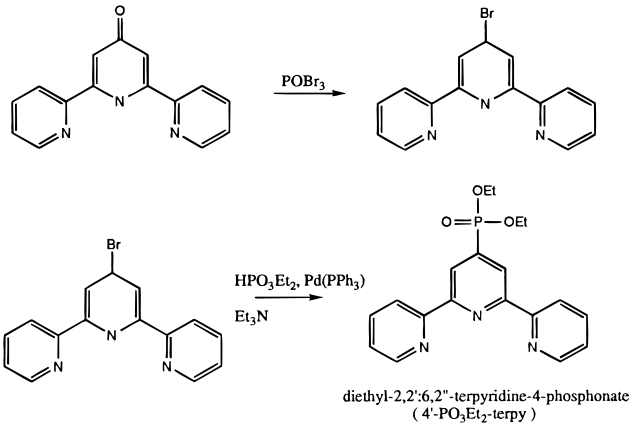

Scheme 2. Synthetic Scheme for Various Ru Complexes Examined in This Work

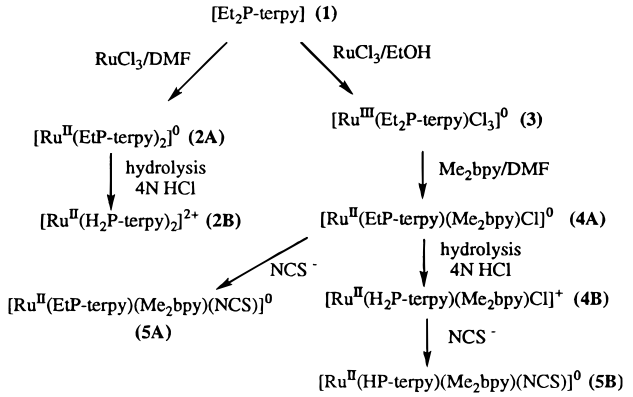

The major focus of this work has been the characterization of polypyridine complexes of Ru(II) with this P-terpy as the key anchoring ligand. Scheme 2 outlines the sequence of reactions employed to obtain various terpyridine complexes examined in this work. As indicated in the scheme, partial hydrolysis of the diester form of the ligand occurred during the high-temperature reflux conditions. The presence of the monoester form of the complexes **2A** and **4A** has been confirmed by ^{1}H and ^{31}P NMR spectral analysis of the products.

The monoester complex [Ru(EtP-terpy)(Me_2bpy)(Cl)] (**4A**) was hydrolyzed using 4 N HCl to prepare the complex [Ru(H_2P-terpy)(Me_2bpy)(Cl)]$^+$ (**4B**). The substitution of the chloride by thiocyanato ligand in the complex **4A** or **4B** was achieved by refluxing in the presence of aqueous NaNCS in DMF:

$$[\mathrm{Ru(H_2P\text{-}terpy)(Me_2bpy)(Cl)}]^+ + \mathrm{NCS}^- \rightarrow [\mathrm{Ru(HP\text{-}terpy))(Me_2bpy)(NCS)} \quad (1)$$

The major focus of this work is on the thiocyanato complexes in view of their usage as photosensitizers. The structures of various isolated complexes have been established by a combination of physical methods. It has also been possible to obtain single crystals of the thiocyanato complex **5B** by slow evaporation of concentrated solutions and establish its crystal structure by X-ray diffraction methods.

(16) Hirao, T.; Masunaga, T.; Ohshiro, Y.; Agawa, T. *Synthesis* **1981**, 56.

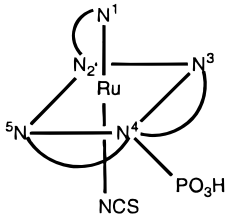

[Ru(HP-terpy)(Me_2bpy)(NCS)] **(5B)**

2. Crystal Structure of the Mixed-Ligand Thiocyanato Complex 5B. Knowledge of the arrangement of the ligands in the complex and in the crystal allows better estimation of the possible orientation of the complex on the semiconductor surface. Single crystals suitable for X-ray diffraction study were grown by slow evaporation of a concentrated solution in DMSO. The single crystal structure of **5B** consists of the neutral complex [Ru(HP-terpy)(Me_2bpy)(NCS)] and solvent molecules dimethyl sulfoxide and water. Figure 1 presents the SEM micrograph of the single crystals examined in this work. The typical platelike shape of the crystals can be readily seen.

Figure 2 presents an ORTEP diagram of the molecular structure of the mixed-ligand complex [Ru(HP-terpy)(Me_2bpy)-(NCS)] as determined by X-ray diffraction data. The measured bond distances (Å) and the bond angles around the central Ru atom are listed in Table 3. The structure of the complex is best described as a distorted octahedron, similar to that observed in structurally related mixed-ligand polypyridyl complexes reported recently:[17−19] $[Ru(terpy)(bpy)(H_2O)]^{2+}$ and $[Os(terpy)-(bpy)(H_2O)]^{2+}$. The three nitrogens of the terpyridine and one N of the bipyridine form one plane, and the second N of the Me_2-bpy and thiocyanate ligand take up the axial positions. The molecular structure observed in the present case appears to be typical of transition metal (d^6) complexes containing one terpyridine (LLL), one bipyridine (LL), and one monodentate ligand (X), [M(LLL)(LL)X] (M = Ru(II) or Os(II). It is interesting to note that the structural details of the three complexes are strikingly similar. Clearly the effect of substituents on the terpy and bpy ligand is very marginal. The NRuN angles span a range (77.7−103.90° instead of 90° and 159.1−176.1° instead of 180°), but the deviations do not exceed the values observed in structurally similar complexes.

The mutual orientation of the ligands in the molecule is shown in Figure 3. The bpy and terpy ligands are nearly planar (the maximum deviations of atoms from the mean planes of the ligands are 0.074 and 0.044 Å) and practically perpendicular to each other (dihedral angle of 89.5°). The terminal methyl groups are deviating essentially from the plane of the bpy ligand (−0.025 Å for C(11) and 0.148 Å for C(12)), while the P-substituent lies exactly in the plane of the terpy ligand (deviation of 0.002 Å). The Ru atom deviates significantly from the mean planes of both ligands (0.075 Å from bpy and 0.060 Å from terpy).

The relative orientation of the thiocyanate group in complex **5B** and its surrounding is of interest, in view of the role of these complexes as photosensitizers and the question of mode of anchoring of these molecules on oxide surfaces. Table 4

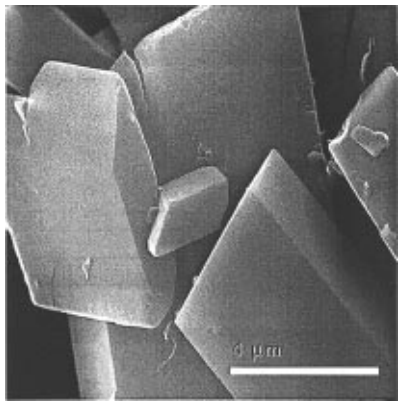

Figure 1. SEM micrograph of single crystals of **5B**.

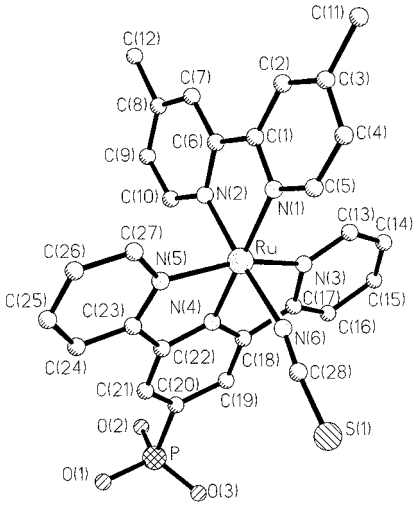

Figure 2. ORTEP diagram showing the molecular structure of the complex [Ru(HP-terpy)(Me_2-bpy)(NCS)]. Hydrogen atoms are omitted for clarity.

presents a comparison of the geometry of the Ru−NCS moiety in the Ru−terpy complex **5B** with complexes containing such N-thiocyanato complexes reported earlier:[20−22] [$(COOEt)_2$-bpy)$(NCS)_2$Ru] (**6**), [Ru(bpy)$(NCS)_2$] (**7**), and Ru(η^5-C_5H_5)-(NCS)$(C_{18}H_{15}P)_2$ (**8**). A broad range of values (130 −180°) have been reported for metal−thiocyanates wherein the metal atoms are N-bonded to pseudohalides.[23] In complex **5B**, the Ru−N(6)−C(28) bond angle is bent up to 165(2)°, in the same range as observed in structurally similar Ru−thiocyanato complexes **7** and **8**. This may indicate a large donation of the dπ-electrons of Ru atom to the π-acceptor thiocyanate ligands.[21] The bond angle N(6)−C(28)−S(1) of 174(2)° indicates the conservation of the linearity of the thiocyanato ligand in complex **5B**. There are no specific intermolecular contacts of the S(1) atoms which could influence the bonding of the thiocyanato group to the Ru atom. The shortest intermolecular contacts of the S(1) atom are S(1)···C(2) 3.67(2) Å to the Me2-bpy ligand, related by the transformation (x, $y + 1$, z) and S(1)···C(26) 3.74 Å and S(1)···C(27) 3.60 Å with the terpy ligand related by the transformation ($1 - x$, $-y$, $1 - z$). The sum of van der Waals radii is 3.50 Å.[24]

(17) (a) Cheng, C. C.; Goll, J. G.; Neyhart, G. A.; Welch, T. W.; Singh, P.; Thorp, H. H. *J. Am. Chem. Soc.* **1995**, *117*, 2970. (b) Roecker, L. E. Ph.D. Thesis, Univ. of North Carolina, Chapel Hill, NC, 1983. (c) Seok, W. K. Ph.D Thesis, Univ. of North Carolina, Chapel Hill, NC, 1988.
(18) Rasmussen, S. C.; Ronco, S. E.; Misna, D. A.; Billadeau, M. A.; Pennington, W. T.; Kolis, J. W.; Petersen, J. D. *Inorg. Chem.* **1995**, *34*, 821.
(19) Shklover, V.; Eremenko, I. L.; Berke, H.; Nesper, R.; Zakeeruddin, S. M.; Nazeeruddin, Md. K.; Grätzel, M. *Inorg. Chim. Acta* **1994**, *219*, 11.
(20) Shklover, V. E.; Nazeeruddin, Md. K.; Zakeeruddin, S. M.; Barbe, C.; Kay, A.; Haibach, T.; Steurer, W.; Hermann, R.; Nissen, H.-U.; Grätzel, M. *Chem. Mater.*, in press.
(21) Herber, R. H.; Nan, G.; Potenza, J. A.; Schugar, H. J.; Bino, A. *Inorg. Chem.* **1989**, *28*, 938.
(22) Booyen, P. H. *Acta Crystallogr.* **1992**, *C48*, 545.
(23) Drew, M. G. B.; bin-Othman, A. H.; Nelson, S. M. *J. Chem. Soc., Dalton Trans.* **1976**, 1394.
(24) Bondi, A. *J. Phys. Chem.* **1964**, *68*, 441.

Table 3. Comparison of Selected Bond Distances and Bond Angles for Complex **5B** with Those of $Ru(terpy)(bpy)(H_2O)]^{2+}$ (**9**) and $Os(terpy)(bpy)(OH_2)]^{2+}$ (**10**)[a]

	5B	**9**[b]	**10**[c]
	Selected Bond Distances (Å)		
M−N(1)	2.06(1)	2.07	2.03
M−N(2)	2.01(1)	2.02	2.02
M−N(3)	2.07(1)	2.05	2.10
M−N(4)	1.94(1)	1.96	1.96
M−N(5)	2.08(1)	2.06	2.05
M−X(6)	2.11(1)	2.13	2.14
	Selected Bond Angles (deg)		
N(1)RuN(2)	77.7(6)	78.1	77.1
N(1)RuN(3)	96.8(6)	99.3	103.3
N(1)RuN(4)	176.1(5)	176.1	176.7
N(1)RuN(5)	103.9(6)	102.0	99.0
N(1)RuX(6)	96.4(6)	96.9	94.6
N(2)RuN(3)	90.3(5)	92.7	92.1
N(2)RuN(4)	99.5(6)	98.1	99.7
N(2)RuN(5)	91.6(6)	93.2	93.7
N(2)RuX(6)	173.9(6)	174.9	171.6
N(3)RuN(4)	80.5(6)	79.8	77.5
N(3)RuN(5)	159.1(6)	158.7	157.7
N(3)RuX(6)	91.5(5)	88.5	86.6
N(4)RuN(5)	78.7(6)	79.1	80.3
N(4)RuX(6)	86.6(6)	86.9	88.6
N(5)RuX(6)	88.7(6)	87.4	92.1

[a] The numbering scheme employed is N(1) and N(2) for the bipyridine nitrogens and N(3), N(4), and N(5) for the terpyridine nitrogen atoms, and X denotes the sixth axial ligand (X = NCS, OH_2). [b] Data for complex $Ru(terpy)(bpy)(H_2O)]^{2+}$ (**9**): Soek, W. K. Ph.D Thesis, Univ. of North Carolina, Chapel Hill, NC, 1988. [c] Data for complex $Os(terpy)(bpy)(OH_2)]^{2+}$ (**10**): Cheng, C.-C.; Goll, J. G.; Neyhart, G. A.; Welch, T. W.; Singh, P.; Thorp, H. H. *J. Am. Chem. Soc.* **1995**, *117*, 2970.

On the equatorial plane, N(1), N(3), N(4), and N(5) are coplanar within 0.008 Å. When considering the bonds Ru−N(2)−N(6) as axial ones, the deviation of the Ru atom from the equatorial plane (defined by N(1), N(3), N(4), and N(5) atoms) is 0.043 Å toward the N(6) atom. There is no weakening of the Ru−N(6) interaction. Had there been a weakening of the interaction, this would be accompanied by the shift of the Ru atom from the equatorial plane toward the N(2) atom, as observed in some cases.[25]

Concerning the anchoring group phosphonate, there are chemically different P−O bonds in the complex **5B**: P═O, P−O$^-$, and P−OH. The very small size of the crystals employed in the structural study work did not permit high precision measurements. Hence only qualitative discussions can be made on the basis of the observed P−O separations: P−O(1), P−O(2), and P−O(3) are 1.51(1), 1.56(1), and 1.46(1) Å, respectively. The corresponding O−O−C(20) bond angles are 105.6(8), 104.0(8), and 109.7°. The above separation suggest P−O(1), P−O(2), and P−O(3) bonds to be indicative of the P−O, P−OH, and P═O type, respectively. The torsional angles OPC(20)C(21) are −3.3, 111.2, and −131.8° for the O(1), O(2) and O(3) bond, respectively. The rotation of the group −P(═O)(OH)(O$^-$) around the C(20)−P bond will be determined by the crystal packing requirements and intermolecular hydrogen bonds. The observed bond length of 1.84(2) Å for the P−C(20) bond is close to values reported for ordinary P−C(ar) bonds 1.801 Å in C_2−P(═O)−C_{ar} or 1.836 Å in C_2−P−C_{ar} moieties.[26] The ordinary character of the P−C(20) bond does not preclude free rotation of the group −P(═O)(OH)(O$^-$) around the P−C(20) bond.

(25) Auf der Heyde, T. In *Structure Correlation*; Bürgi, H.-B., Dunitz, J. D., Eds.; VCH Publishers: New York, 1994; Vol. 1, p 337.
(26) Allen, F. H.; Kennard, O.; Watson, D. G.; Brammer, L.; Orpen, A. G. *J. Chem Soc., Perkin Trans. 2* **1987**, S1.

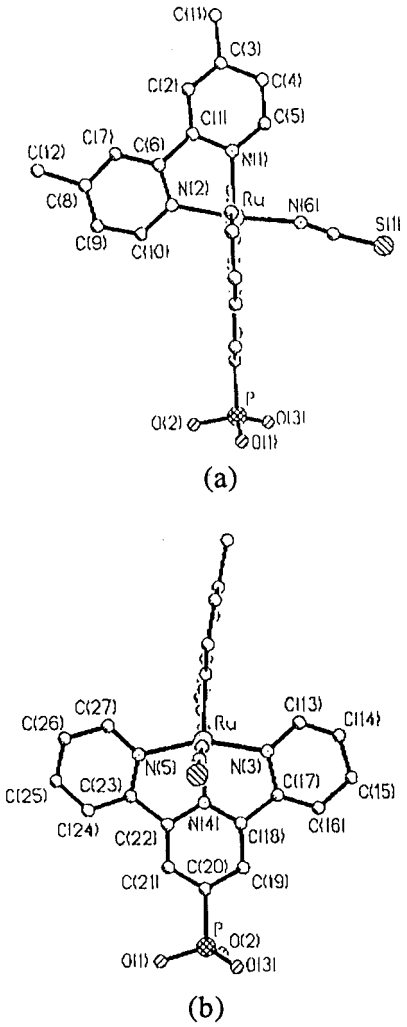

Figure 3. Mutual orientation of the ligand in the complex **5B**: (a) projection on the plane of the bpy ligand; (b) projection on the plane of the terpy ligand.

Table 4. Comparison of Structural Parameters of the Thiocyanato Moiety in Various (Thiocyanato-*N*)ruthenium Complexes[a]

complex	Ru−N(NCS) (Å)	Ru−N−C(S) (deg)	N−C−S (deg)	ref
5B	2.11(1)	165(2)	176(1)	this work
6	2.07(2)	174(2)	178(2)	4
7	2.055(5)	168.2(5)	177.5(6)	5
8	2.070(4)	168.4(5)	178.7(6)	6

[a] Complexes **6**−**8** are $Ru(4,4'\text{-}COOEt\text{-}2,2'\text{-}bpy)_2(NCS)_2$ (**6**), $Ru(2,2'\text{-}bpy)_2(NCS)_2$ (**7**), and $Ru(\eta^5\text{-}C_5H_5)(NCS)(C_{18}H_{15}P)_2$ (**8**), respectively.

3. ^{1}H NMR Spectra. The ^{1}H NMR spectral data obtained for the free ligand and the complexes were summarized in Table 5. Complex **5B** shows sharp and well-resolved signals in the aromatic region, corresponding to pyridyl protons. In an octahedral/pseudo-octahedral geometry, a tridentate ligand like terpyridine coordinates to the metal center in meridional fashion and the bidentate ligand occupies an orthogonal plane. In this configuration, the two rings of 4,4-dimethyl-2,2′-bipyridine are located in such a way that one ring is in the plane and the other half is above the plane and therefore exhibits six resonances in the aromatic region. In complex **5B**, the proton assignments of the phosphonated terpyridine and 4,4-dimethylbipyridine were made on the basis of coupling constants and the peak integration in the aromatic region.

The lowest field doublet centered at δ 9.38 ppm is assigned to the H6 proton of the 4,4-dimethyl-2,2′-bipyridine ring, which is *cis* to the NCS$^-$ group. The remaining singlet at δ 8.71 ppm

Table 5. ^{1}H NMR (200 MHz) Spectral Data for Ligands (in $CDCl_3$) and Ru Complexes (in DMSO-d_6)

ligand/complex	^{1}H NMR data (ppm)
4-bromo-terpy	7.38 (ddd, 2H, 7.6, 4.9, 1.2 Hz), 7.88 (dt, 2H, 7.9, 1.8 Hz), 8.59 (dt, 2H, 7.9, 0.9 Hz), 8.66 (s, 2H), 8.72 (ddd, 2H, 4.9, 1.8, 0.9 Hz)
4′-PO_3Et_2-terpy **(2)**	1.35 (t, 6H, 7 Hz), 4.21 (m, 4H), 7.30 (ddd, 2H, 7.5 Hz, 5 Hz, 2 Hz), 7.82 (dt, 2H, 8 Hz, 2 Hz), 8.56 (d, 2H, 8 Hz), 8.68 (d, 2H, 4.5 Hz), 8.82 (d, 2H, $^3J_{P-H} = 14$ Hz)
[Ru(EtP-terpy)$_2$] **(2A)**	1.26 (t, 3H), 3.99 (q, 2H), 7.26 (t, 2H), 7.37 (d, 2H), 7.96 (t, 2H), 8.92 (d, 2H), 9.04 (d, 2H)
[Ru(H_2P-terpy)$_2$]Cl_2**(2B)**[a]	7.13 (t, 2H, 5.2 Hz), 7.37 (d, 2H, 4.8 Hz), 7.90 (t, 2H, 5.9 Hz), 8.57(d, 2H, 5.7 Hz), 8.96 (d, 2H, $^3J_{P-H}$ =12.1 Hz)
[Ru(EtP-terpy)(Me_2bpy)(Cl)] **(4A)**	2.30 (s, 3H), 2.75 (s, 3H), 6.88 (d,1H, 5.0 Hz), 7.07 (d,1H, 5.80 Hz), 7.39 (t, 2H, 6.5 Hz), 7.63 (d, 2H, 5.0 Hz), 7.94 (t, 3H), 8.51 (s, 1H), 8.72 (s, 1H), 8.78 (d, 2H, 7.4 Hz), 8.89 (d, 2H, $^3J_{P-H} = 12.7$ Hz), 9.90 (d, 1H, 5.8 Hz)
[Ru(EtP-terpy)(Me_2bpy)(NCS)] **(5A)**	2.35 (s, 3H), 2.80 (s, 3H), 6.90 (d, 1H, 5.8 Hz), 7.06 (d, 1H, 5.8 Hz), 7.45 (t, 2H, 7.0 Hz), 7.79 (d, 2H, 5.0 Hz), 7.95 (t, 3H), 8.45 (s, 1H), 8.68 (s, 1H), 8.73 (d, 2H, 6.0 Hz), 8.80 (d, 2H, $^3J_{P-H} = 11$ Hz), 9.50 (d, 1H, 6 Hz)
[Ru(H_2Pterpy)(Me_2bpy)(Cl)]Cl **(4B)**	2.31 (s, 3H), 2.75 (s, 3H), 6.90 (d, 1H, 4.6 Hz), 7.08 (d, 1H, 5.9 Hz), 7.41 (t, 2H, 5.9 Hz), 7.64 (d, 2H, 4.7 Hz), 8.06 (t, 3H), 8.51 (s, 1H), 8.74 (s, 1H), 8.79 (d, 2H, 3.2 Hz), 8.85 (d, 2H, $^3J_{P-H} = 12.9$ Hz), 9.90 (d, 1H, 5.8 Hz)
[Ru(HP-terpy)(Me_2bpy)(NCS)] **(5B)**	2.31 (s, 3H), 2.74 (s, 3H), 6.99 (d, 1H, 5.8 Hz), 7.06 (d, 1H, 5.8 Hz), 7.39 (t, 2H, 6.4 Hz), 7.65 (d, 2H, 5.0 Hz), 7.98 (t, 3H), 8.50 (s, 1H), 8.71 (s, 1H), 8.76 (d, 2H, 6.8 Hz), 8.95 (d, 2H, $^3J_{P-H} = 10.8$ Hz), 9.38 (d, 1H, 5.8 Hz)

[a] In D_2O.

and the doublet centered at δ 8.76 ppm may thus be assigned to the H3 and H5 protons, respectively. The high-field singlet at δ 8.51 and two doublets centered at δ 7.65 and 6.99 ppm due to the H3′, H5′, and H6′ protons, respectively, are *trans* to the NCS ligand. The resonance signal of the H6′ proton of the pyridine ring is significantly upfield shifted when compared to the free ligand. This shielding effect on the H6′ proton may be due to ring currents of the terpyridine ligand, which is in the plane.[27] In the aliphatic region there are two singlets at δ 2.31 and 2.74 ppm corresponding to the methyl protons of magnetically nonequivalent two pyridine rings of 4,4-dimethylbipyridine.

The most characteristic feature of the central pyridine H3 proton of the phosphonated terpyridine ligand is its coupling with the phosphorus, which gives a doublet centered at δ 8.95 (10.8 Hz). The terminal pyridines show two doublets and two triplets centered at δ 8.76, 7.65, 7.98, and 7.39 assigned to H3″, H6″, H4″, and H5″, respectively.

^{31}P NMR Spectra. ^{1}H and ^{13}C NMR data for transition metal complexes of polypyridyl ligands have been used by many authors to study the interaction between the ligands and the metal. The formation of a bond between a metal and a ligand is viewed as a result of σ donation and the π-back-bonding. Qualitative analyses of the σ donation and π back-bonding and the steric effects in transition metal complexes containing phosphine ligands have been performed by several groups.[28] However in polypyridyl complexes a qualitative description of the σ bonding and π back-bonding has not been addressed. For the first time we use phosphorus NMR data for phosphonated polypyridyl ligands to interpret σ and π donor effects in transition metal complexes.

The ^{31}P chemical shifts of the free ligand and the Ru complexes may serve as useful sensors to monitor the electronic charge density distribution upon formation of the complexes. The ^{31}P of the free ligand PPh_3, for example, shifts from -5 to 41 ppm upon formation of a $Ru(PPh_3)_2(Cl)_2$ complex.[29] The 46 ppm downfield shift upon complexation is due to the direct coordination of PPh_3 ligand to the metal. This clearly shows the extensive charge flow from ligand to the Ru metal center. Table 6 presents data on the observed ^{31}P NMR chemical shifts for various phosphonated-terpyridine complexes. The phosphorus resonance peak is more sensitive to pH due to the protonation and the deprotonation of the phosphonate group. Because of this reason we compare the phosphorus NMR data for the free ligand and complexes measured in alkaline D_2O, where the phosphonate group is completely ionized.

Table 6. ^{31}P-NMR Chemical Shifts of Various Phosphonated terpy Complexes Measured in Solution at Room Temperature

complex	solvent	chem. shift
Et_2P-terpy (**1**)	DMSO	15.14
H_2P-terpy	DMSO	9.51
[Ru(EtP-terpy)$_2$] (**2A**)	DMSO	8.28
[Ru(EtP-terpy)(Me_2bpy)(Cl)] (**4A**)	DMSO	4.61
[Ru(H_2P-terpy)(Me_2bpy)(Cl)] (**4B**)	DMSO	8.56
[Ru(EtP-terpy)(Me_2bpy)(NCS)] (**5A**)	DMSO	6.90
[Ru(HP-terpy)(Me_2bpy)(NCS)] (**5B**)	DMSO	3.08
P-terpy^{2-}	alk[a] D_2O	7.93
[Ru(P-terpy)$_2$]$^{2-}$ (**2B**)	alk D_2O	7.23
[Ru(P-terpy)$^{2-}$(Me_2bpy)(NCS)]	alk D_2O	7.35

[a] alk = alkaline.

The ^{31}P NMR spectrum of the H_2P-terpy ligand shows a resonance peak at 7.93 ppm, with respect to an external standard 85% H_3PO_4. Upon coordination to the ruthenium center this line moves from 7.93 to 7.23 and 7.35, in complexes **2B** and **5A,** respectively. The ~0.7 ppm upfield shift is opposite to that observed for the PPh_3 case. The upfield shift reflects the extent of π back-bonding capacity of the phosphonated terpyridine ligand in these complexes. The large difference in the chemical shift between **5A** and the $Ru(PPh_3)_2(Cl)_2$ complex could be due to the fact that the triphenylphosphine is directly involved in the coordination to the metal whereas, in phosphonated terpyridine, it is a secondary effect on the phosphorus.

The ^{31}P line of H_2P-terpy ligand in DMSO-d_6 moves from 9.51 to 8.56 ppm upon formation of the [Ru(H_2P-terpy)(Me_2bpy)(Cl)]$^+$ complex. With replacement of the chloride ligand by NCS, in complex **5B**, the ^{31}P peak moves to 3.08 ppm. The downfield shift of more than 5 ppm, compared to the chloro complex, reflects the π-acceptor capacity of the thiocyanato ligand.

^{13}C NMR Spectra. The ^{13}C{^{1}H} NMR spectrum of complex **5B** shows 18 resonance signals in the aromatic region (δ 160−123 ppm) corresponding to 4,4′-dimethyl-2,2-bipyridine and 4-phosphonated terpyridine. No attempts were made to assign all the signals. The two resonance peaks in the aliphatic region, at δ 20.87 and 20.31 ppm, correspond to two nonequivalent methyl carbon atoms of 4,4′-dimethyl-2,2-bipyridine. The interesting feature of the ^{13}C NMR spectrum is the presence of a sharp resonance peak at δ 137.67 ppm, which we assign to the N-coordinated NCS carbon atom.[21]

IR Spectra. The infrared spectra of the ligand and the complex were recorded in KBr pellets in the 4000−250 cm^{-1} region. The most direct evidence for the presence of N-coordinated NCS comes from the IR spectra. The strong absorption band at 2110 cm^{-1} is assigned as to the N-bonded NCS^- ligand ν(C═N) stretching vibration. The presence of band at 785 cm^{-1} is assigned to the ν(C═S) stretching vibration. The free ligand has three characteristic stretching bands corre-

(27) Orellana, G.; Ibarra. C. A.; Santoro, J. *Inorg. Chem.* **1988**, *27*, 1025.
(28) Neal Golovim, M.; Matiur Rahman, Md.; Balmonte, J. E.; Giering, W. P. *Organometallics* **1985**, *4*, 1981.
(29) Hoffman, P. R.; Coulton, K. G. *J. Am. Chem. Soc.* **1975**, *97*, 4221.

Table 7. Ground-State Resonance Raman Frequencies (cm^{-1}) of Phosphonated terpy Complexes of Ru

2A in H_2O	P-terpy **1** in H_2O	**5A** in H_2O	**5A** in DMSO	Ru-$(DMB)_3^{2+}$ [32]	Ru-$(bpy)_3^{2+}$ [32]	assgnt
		1619	1615	1619		DMB
1610	1596	1602	1599		(1605)	PO_3-terpy
1566	1568	1560				PO_3-terpy
	1543	1549	1541	1552	(1557)	DMB?
1536		1520	1526			PO_3-terpy
1476	1479	1473	1476	1481	(1487)	DMB/PO_3-terpy
1419		*1414*	*1415*			
1400		1393				PO_3-terpy
1350	1337	1340	1340			PO_3-terpy
		1322	1321	1316	(1316)	DMB
1291	1288	1285				PO_3-terpy
1273		1269		1274	(1274)	DMB/PO_3-terpy
		1255	1254	1258	(1254)	DMB
1246	1244	1248				PO_3-terpy
		1200	1198	1197		DMB
1166	1155	1166	1161		(1170)	PO_3-terpy
1142		1137	1134	1146		DMB/PO_3-terpy
1056	1045		1053		(1041)	
1024	1000		1020	1025	(1023)	DMB
	973	947	983			
826		811				
	792	785			(766)	
				742	(728)	DMB
690						
655			659		(664)	
	622					
578			559	576		DMB

sponding to ν(P−O) at 1250, 1170, and 990 cm^{-1}. In the complex **5B**, the bands are observed at 1240, 1140, and 975 cm^{-1}. The slight decrease in the energy of the P−O stretching vibrations is due to the delocalization of electron density upon coordination to the metal center.

4. Resonance Raman Spectral Studies. Resonance Raman spectroscopy is a powerful technique for identification of lowest energy CT in mixed-ligand complexes. Excitation into an allowed M → π^*_{LL} transition gives rise to enhancement of the normal modes most intimately coupled to the electronic transition in resonance. In a broad absorption band consisting of several overlapping CT transitions (as in the present case) the relative contribution of each transition at a given wavelength can be determined by studying the wavelength dependence of the resonance enhancement of the bands corresponding to different ligands (LLL, LL). There have been a number of such studies on the polypyridyl complexes.[30−33] In the present work, the homo bis-chelates are used to establish the marker bands of the phosphonated terpyridine and subsequently this information is used to establish the nature of the lowest energy excited state in the mixed ligand complexes involving this ligand.

Table 7 presents a summary of the various Raman bands observed for complexes **1**, **2A**, **5A**, and **5B** measured in aqueous solutions. On the basis of a comparison of the results obtained for various mixed-ligand systems and the free ligand itself, Raman bands at ≈1610, 1536, 1400, 1350, 1291, and 1246 cm^{-1} can be considered as "marker" bands of the phosphonated terpy ligand. Earlier studies[32] have identified the marker bands of

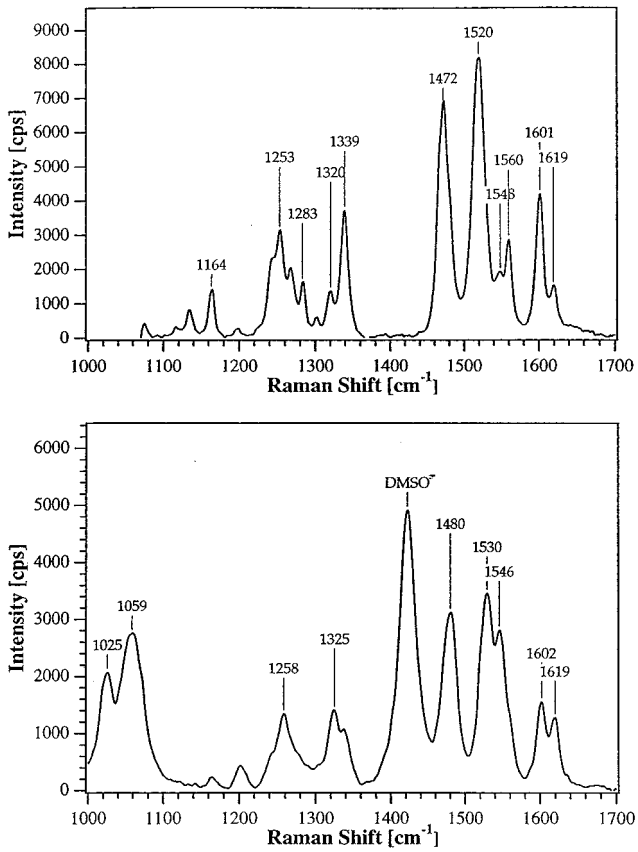

Figure 4. Resonance Raman spectra of the mixed-ligand complex **5B**, [Ru(HP-terpy)(Me_2bpy)(NCS], in aqueous solution for two different excitation wavelengths of 514.5 nm (top) and 457.9 nm (bottom).

Me_2bpy ligand to appear at 1619, 1549, 1316, and 1254 cm^{-1}, respectively. With the information on the marker bands characteristic of the two ligands involved in the CT transitions in the visible region, it is possible to probe their relative intensities for excitation at two different wavelengths within the broad absorption band. In mixed complexes **5A**,**B**, there are potentially two candidates for the lowest energy MLCT transition: Ru → Me_2bpy (bidentate ligand) and Ru → P-terpy (tridentate). A priori, the energy levels of these transitions are expected to be very similar. Using electrochemical data alone, it is not possible to identify the lowest energy excited state that is responsible for the observed luminescence and photoredox properties. This assignment is important, in view of the important role they play in influencing the excited-state properties (luminescence lifetime, intensity, etc.). In mixed-ligand complexes, it is useful to know which of the coordinating ligands is intimately involved in the metal-to-ligand charge transfer. The efficiency of charge injection from the excited state can be different if that particular ligand carrying the anchoring group is not directly with the MLCT excitation process.

Figure 4 presents the resonance Raman spectra of complex **5B** observed upon excitation at two wavelengths 514.5 and 457.9 nm. The former wavelength is at the tail end of the absorption band and is very likely to be associated with the lowest energy MLCT transition. It is instructive to compare the relative intensity for the pair of Raman bands at 1602, 1620; 1520, 1548; and 1320 and 1340 cm^{-1}. The marker bands of HP-terpy are more intensity enhancement for excitation at 514 nm while that of the Me_2-bpy are intense for 454 nm excitation. Clearly the low-energy absorption is dominated by contributions coming from Ru → P-terpy CT. Hence, the lowest energy excited state in the mixed-ligand complex can be assigned to be Ru → P-terpy in character.

(30) Nazeeruddin, Md. K.; Grätzel, M.; Kalyanasundaram, K.; Girling, R. B.; Hester, R. E. *J. Chem. Soc., Dalton Trans.* **1993**, 323.
(31) Hage, R.; Haasnoot, J. G.; Stufkens, D. J.; Snocek, T. L.; Vos, J. G.; Reedjik, J. *Inorg. Chem.* **1989**, *28*, 1413. Knorrs, C.; Gafney, H. D.; Baker, A. D.; Braunstein, C.; Strekas, T. C. *J. Raman Spectrsc.* **1983**, *14*, 32. Yabe, T.; Orman, L. K.; Anderson, D. R.; Yu, S.-C.; Xu, X.; Hopkins, J. B. *J. Phys. Chem.* **1990**, *94*, 7128.
(32) Mabrouk, P. A.; Wrighton, M. S. *Inorg. Chem.* **1986**, *25*, 526. Orman, L. K.; Chang, Y. J.; Anderson, D. R.; Yabe, T.; Xu, X.; Yu, S-C.; Hopkins, J. B. *J. Chem. Phys.* **1989**, *90*, 1469.
(33) Danzer, G. D.; Kincaid, J. R. *J. Phys. Chem.* **1990**, *94*, 3976. Kumar, C. V.; Barton, J. K.; Gould, I. R.; Turro, N. J.; Van Houten, J. *Inorg. Chem.* **1988**, *27*, 648.

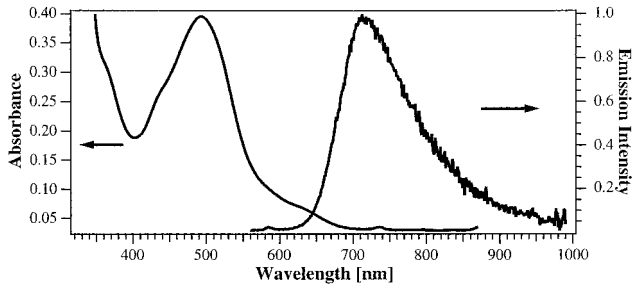

Figure 5. Absorption and emission spectra of the mixed-ligand complex **5B** in ethanolic solutions at room temperature.

Table 8. Absorption and Luminescence Properties of Ru Complexes Containing Phosphonated-terpy Ligands in Room-Temperature Fluid Solutions

complex/solvent	abs max (nm) (ϵ (M^{-1} cm^{-1}))	emission max (nm)	emission quantum yield	emission lifetime (ns)
2B/water	480 (12 500)	643	2.4×10^{-5}	2.0
5A/DMSO	500 (9500)	718	2×10^{-4}	
5A/EtOH	506 (9000)	780	5.8×10^{-4}	29
5B/DMSO	494 (8700)	712	6×10^{-4}	25
5B/EtOH + 10% DMSO	494 (8500)	708	4.4×10^{-4}	15
$[Ru(terpy)_2]^{2+}/CH_3CN$[a]	474 (10 400)	629	$\leq 5 \times 10^{-6}$	?
$[Ru(MeSO_2\text{-}terpy)_2]/CH_3CN$[a]	486 (21 100)	666	5×10^{-4}	25.0

[a] Data taken from ref 5.

5. UV−Visible Absorption, Emission, and Redox Potentials. The homo bis and the mixed-ligand chelates are highly colored (orange red), due to moderately intense metal-to-ligand charge transfer (MLCT) transitions in the visible light region. Table 8 presents data on the absorption and luminescence properties of several P-terpy complexes in fluid solution at room temperature. Figure 5 presents the representative absorption and emission spectra for the mixed-ligand thiocyanato complex **5B**. The bis(P-terpy) complex (**2B**) has the maximum at 480 nm (in water), slightly red-shifted (by ca. 5 nm) with respect to the parent/unsubstituted $[Ru(terpy)_2]^{2+}$ complex.[5,34] In $[Ru(terpy)_2]^{2+}$, the MLCT maximum is at 475 nm ($\epsilon \approx 10\,400$ M^{-1} cm^{-1}) and a weak emission with maximum at 630 nm.[5] Thus, the effect of phosphonate insertion on the absorption and redox properties of the parent $[Ru(terpy)_2]^{2+}$ appears to be very marginal. It is much less than what has been reported earlier for the analogous complex with 4′-($MeSO_2$)-substituted terpyridine derivative.[5]

In the mixed-ligand complex [Ru(HP-terpy)(Me_2bpy)(NCS)] (**5B**), the MLCT maximum further red-shifts to ≈498 nm (ϵ = 8500 M^{-1} cm^{-1} in ethanol). Intraligand $\pi-\pi^*$ transitions of P-terpy are located at 320 nm, while that of Me_2bpy is at 280 nm. The broad absorption in the intermediate range (400−500 nm) is a composite of MLCT transitions involving P-terpy and Me_2bpy ligands. Very similar absorption properties of the monoester **5A** (maxima at 500 nm (ϵ = 10 000 M^{-1} cm^{-1})) suggest that esterification hardly influences the MLCT transition. In $[Ru(terpy)_2]^{2+}$, the first oxidation and reduction potentials are located at 1.26 and −1.32 (vs SCE) in acetonitrile. Electrochemical studies of complex **5B** in DMSO (containing tetrabutylammonium as support electrolyte) indicate the oxidation and reduction potentials at +0.86 and −1.37 V vs SCE, respectively. When compared to the $Ru(terpy)_2$ complex, the oxidation potential in complex **5B** is 0.42 V anodically shifted. The decrease in the oxidation potential of complex **5B** could be due to the electron-donating nature of the thiocyanato ligand. The 0.15 V cathodic shift in the reduction potential of complex **5B** compared to $[Ru(terpy)_2]$ complex is consistent with the low oxidation potential of complex **5B**. The presence of the NCS^- group also influences the positions of MLCT transitions; in **5B** it is 20 nm more red-shifted than **2B**.

Identification of the ligand involved in the lowest energy MLCT transition is essential for the assignment of the emission and in the design of photosensitizers for nanocrystalline solar cells based on TiO_2 films. On the basis of the wavelength dependence of resonance Raman spectra of the mixed-ligand complex, it was concluded that the lowest excited state involves Ru → P-terpy CT. Thus the nature of the excited state is similar in both the homo and mixed-ligand chelates examined in this work. The emission quantum yield and lifetimes increase substantially as compared to the parent bis-complexes.

It is interesting to note that, for the mixed-ligand thiocyanato complex with a red-shifted absorption, luminescence showed enhanced emission lifetime and quantum yields. This behavior is rather counterintuitive within the framework of "energy gap law" behavior exhibited by a large number of polypyridyl complexes of Ru. As per the energy gap law, in a homologous series of complexes, the emission intensity and lifetimes decrease with lowering of the energy of the MLCT excited state. This is caused by the increased role played by nonradiative decay processes. The behavior however is consistent with that reported recently for a series of Ru(II) complexes with 4′-substituted 2,2′:6′,2″-terpyridine complexes.[5] In a study involving 14 mixed-ligand complexes, it was observed that (i) both electron-donating and electron-withdrawing substituents caused red-shifts in the absorption and emission and (ii) electron-withdrawing groups increased the luminescence quantum yield, whereas electron-donating substituents showed an opposite effect. The present data reinforce the proposed explanations, viz., decreased role of the upper MC excited state in deactivation processes.

6. Phosphonated terpy Complexes of Ru as Sensitizers for Solar Cells. In earlier publications from this laboratory and elsewhere, it was shown that Ru complexes containing carboxy-substituted bipyridine ligands serve as excellent photosensitizers in the thin-film form of photoelectrochemical solar cells.[8−11,35−38] These cells employ a highly porous few micron-thick semiconducting oxide film of TiO_2 as the substrate for distribution of the dye and as electron acceptor for the primary excited-state charge injection process. Figure 6 presents the photocurrent action spectrum for the sensitization of nanocrystalline TiO_2 films by the mixed-ligand complex **5B**. A monolayer of the dye was adsorbed by dipping a porous 8-μm thick membrane film of TiO_2 in warm stock solutions in ethanol as described earlier.[11] As in earlier studies, the efficiency of charge injection from the excited state is given by the incident-photon-to-current-efficiency (IPCE) values. The IPCE values quoted are for (I^-/I_3^-) as the redox couple in acetonitrile and a TCO counter electrode covered with a transparent film of Pt. The cell was operated in the short circuit mode, and the IPCE values are uncorrected (values based on incident photon flux).

(34) Constable, E. C.; Cargill Thompson, A. M. W.; Tocher, D. A.; Daniels, M. A. M. *New J. Chem.* **1992**, *16*, 855.

(35) Argazzi, R.; Bignozzi, C. A.; Heimer, T. A.; Castellano, F. N.; Meyer, G. J. *Inorg. Chem.* **1994**, *33*, 5741. Heimer, T. A.; Bignozzi, C. A.; Meyer, G. J. *J. Phys. Chem.* **1993**, *97*, 11987.

(36) Knödler, R.; Sopka, J.; Harbach, F.; Grünling, H. W. *Solar Energy Mater. Solar Cells* **1993**, *30*, 277.

(37) Hagfeldt, A.; Didriksson, B.; Palmquist, T.; Lindström, H.; Södergren, S.; Rensmo, H.; Lindquist, S.-E. *Solar Energy Mater. Solar Cells* **1994**, *31*, 481.

(38) Eichberger, R.; Willig, F. *Chem. Phys.* **1990**, *141*, 159. Yan, S. G.; Hupp, J. T. *J. Phys. Chem.* **1996**, *100*, 6867. Moser, J.-E.; Grätzel, M.; Durrant, J. R.; Klug, D. R. In *Femtochemistry: Ultrafast Chemical and Physical Processes in Molecular Systems*; Chirgui, M., Ed.; World Scientific: Singapore, 1996. Rehm, J. M.; McLendon, G. L.; Nagasawa, Y.; Yoshihara, K.; Moser, J.; Grätzel, M. *J. Phys. Chem.* **1996**, *100*, 9577.

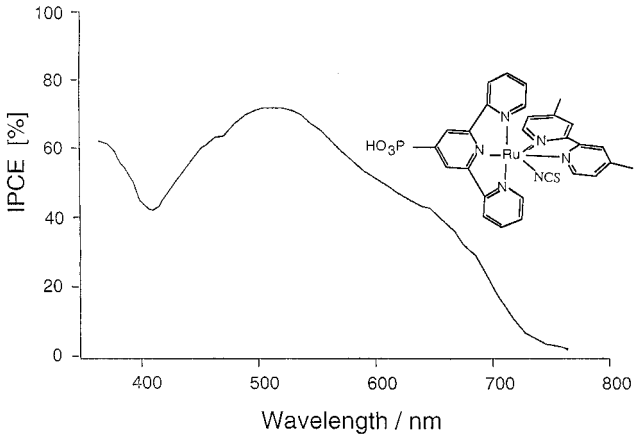

Figure 6. Photocurrent action spectrum for the sensitization of nanocrystalline TiO_2 films by the mixed-ligand complex **5B**. IPCE values quoted are for I^-/I_3^- as the redox couple in acetonitrile and a TCO counter electrode covered with a transparent film of Pt. The cell was operated in the short circuit mode and the IPCE values are uncorrected (values based on incident photon flux).

Quantitative studies of dye adsorption showed that the dye adsorption follows a Langmuir type adsorption isotherm. The adsorption is much better for the phosphonated complex as compared to the analogous carboxybipyridine complex investigated earlier (adsorption constant $= 8 \times 10^6$, a value ca. 80 times larger than that for the dcbpy complex). High IPCE values for monochromatic excitation in the region of the MLCT absorption maximum of the complex attest to efficient charge injection taking place in the phosphonated terpyridine complex as well.

Normally, in dye-sensitized processes, the photocurrent action spectrum reproduces the dye absorption spectrum, except for small changes caused by the derivatization of the dye on the electrode. Most often, such strong resemblance between the absorption spectrum and the photocurrent response is taken as evidence for the direct involvement in the charge injection processes. Careful comparison of the photocurrent action spectrum measured on nanocrystalline oxide semiconductor electrodes with the absorption spectrum of the dye (in solution and also on electrodes) shows that the photocurrent output is considerably higher in the low-energy region. At 700 nm, for example, the absorption of the bis(thiocyanato) complex [Ru(dcbpy)$_2$(NCS)$_2$] is hardly 10% of the maximum value corresponding to 530 nm. Yet the IPCE value at 700 is nearly half.

One possibility is that the dye undergoes substantial structural changes upon derivatization onto the oxide surface leading to different spectral response than that warranted by the solution absorption. In the present case, this appears not to be case. The dye can be extracted out from the oxide surface using alkaline solvents, and the recovered dye does not show any changes in the spectral and luminescence behavior as a result of adsorption to the oxide surface. By controlling the method of preparation of the oxide colloid and the method of deposition, it is possible to prepare nanocrystalline TiO_2 electrodes with varying light scattering/reflecting properties—from transparent to opaque films. Studies using these different forms of oxide films with the same dye sample preparation showed that the photocurrent response in the low-energy region critically depended on the nature (scattering properties of the film).

Taking advantage of the large surface area available in these compact porous films, it is possible to make intensely colored oxide films—layers where the absorbance over few micron thickness of the film exceeds 2 in the region of the maximum of the dye absorption. In the wavelength region where the dye absorption is maximal, the high absorbance values (>2) leads to total extinction of the light within the film while, in the low-energy side, a significant part of the incident radiation penetrates the layer. Multiple reflections of the light in highly scattering films results in increased light absorption and hence increased photoresponse compared to what the solution absorption spectrum indicates. This dependence of the red light response indeed has been verified by incorporation of added scattering centers (μm-size rutile particles of Fluka) during the preparation of the transparent TiO_2 films.[39] In quantitative studies, a shiny Pt mirror was used to reflect the light back, and IPCE values were measured with and without Pt mirror. It has been possible to calculate quantitatively the increased photoresponse in the red using the data absorption properties of the TiO_2 layer, the dye, the redox electrolyte, and the reflective mirror.[40] In fact, in current efforts of dye design, particular attention is being paid to small but definitive absorption tail extending further into the red/near-IR region. It is our hope that, by appropriate "optical engineering", it should be possible to maximize the photocurrent even in the region where the dye absorption is rather small.

Conclusions

The present work, an attempt toward extending the use of 4-substituted terpy complexes of Ru as photosensitizer, has been largely successful. Resonance Raman spectral studies allowed identification of the marker bands characteristic of this new ligand and identification of the lowest excited state in derived Ru complexes. The lowest MLCT of homo and mixed-ligand complexes of phosphonate-substituted terpyridine examined in this work, all of Ru → P-terpy, are luminescent and redox active. The X-ray crystal structure of the thiocyano complex allowed identification of the structural forms taken by Ru complexes of the type [Ru(LLL)(LL)(X)], where LLL, LL, and X stand for the substituted terpyridine, bipyridine, and a monodentate ligand. The high charge injection efficiencies obtained in the nanocrystaline solar cells, particularly in the red region, provide encouragement and hopes for identification of near-infrared-active photosensitizers.

Acknowledgment. We acknowledge financial support of this work by the Swiss National Funds for Scientific Research (FNRS), the Swiss Federal Office for Energy (OFEN), and the National Institute for Applied Photovoltaic Research (INAP), Gelsenkirchen, Germany, and electrochemical experimental assistance from Dr. Nicholas Vlachopoulos.

IC970008I

(39) Barbé, C. J.; Arendse, F.; Comte, P.; Jirousek, M.; Lenzmann, F.; Shklover, V.; Grätzel, M. *J. Am. Ceram. Soc.*, in press.
(40) Papageorgiou, N.; Humphry-Baker, R.; Nazeeruddin, Md. K.; Grätzel, M. To be submitted for publication.